Interhemispheric Asymmetry in the Transient Response of a Coupled Ocean–Atmosphere Model to a CO_2 Forcing

K. BRYAN, S. MANABE AND M. J. SPELMAN

Geophysical Fluid Dynamics Laboratory/NOAA, Princeton University, Princeton, New Jersey

(Manuscript received 5 May 1987, in final form 8 December 1987)

ABSTRACT

Numerical experiments are carried out using a general circulation model of a coupled ocean–atmosphere system with idealized geography, exploring the transient response of climate to a rapid increase of atmospheric carbon dioxide. The computational domain of the model is bounded by meridians 120 degrees apart, and includes two hemispheres. The ratio of land to sea at each latitude corresponds to the actual land–sea ratio for the present geography of the Earth. At the latitude of the Drake Passage the entire sector is occupied by ocean.

In the equivalent of the Northern Hemisphere the ocean delays the climate response to increased atmospheric carbon dioxide. The delay is of the order of several decades, a result corresponding to previous modeling studies. At high latitudes of the equivalent of the ocean-covered Southern Hemisphere, on the other hand, there is no warming at the sea surface, and even a slight cooling over the 50-year duration of the experiment. Two main factors appear to be involved. One is the very large ratio of ocean to land in the Southern Hemisphere. The other factor is the very deep penetration of a meridional overturning associated with the equatorward Ekman transport under the Southern Hemisphere westerlies. The deep cell delays the response to carbon-dioxide warming by upwelling unmodified waters from great depth. This deep cell disappears when the Drake Passage is removed from the model.

1. Introduction

The direct effect of carbon dioxide in the atmospheric radiation balance is perhaps the best understood aspect of the overall CO_2/climate problem. The extreme complexity of predicting the corresponding response of climate is due to the many feedbacks which can take place in the climate system. For example, warming causes an increase of water vapor in the atmosphere, which in turn increases the greenhouse effect (Manabe and Wetherald 1967). It has also been suggested (Hansen et al. 1984) that the carbon dioxide-induced change in cloudiness will provide a positive feedback. Manabe and Bryan (1985) have recently shown that changes in the transport of heat by ocean currents at high latitudes can provide another positive feedback. While much remains to be done in exploring all the feedbacks related to the equilibrium response of climate to atmospheric carbon dioxide variations, the present study is focused on an even less well understood aspect: the *transient* response of climate to an increase of greenhouse gases. The transient response of climate is strongly controlled not only by the feedbacks identified above, but also by the very large thermal inertia of the ocean.

Corresponding author address: Dr. Kirk Bryan, Geophysical Fluid Dynamics/NOAA, Princeton University, P.O. Box 308, Princeton, NJ 08542.

The heat capacity of the upper three meters of the ocean is greater than the entire heat capacity of the atmosphere. The rate at which the climate system will change therefore depends on how rapidly heat anomalies generated in the atmosphere penetrate down into the ocean. The immediate focus of this study is an attempt to gain an understanding of the processes involved, with the precise quantitative prediction of this process as a long-term goal. Two extreme cases can be visualized. In one case no penetration of the ocean takes place, and the atmosphere would respond fully to carbon dioxide increases within a period of years. The other extreme case would be a complete mixing of any heat anomalies through the entire depth of the ocean. Mixing to the ocean bottom would imply such an enormous thermal inertia in the climate system that even a partial response to a sudden increase of atmospheric carbon dioxide would require centuries. In the Northern Hemisphere transient tracers like bomb-produced tritium, and bomb-produced carbon-14 indicate that the intensity of vertical mixing of the ocean is between these extreme cases. Surface properties mix downward into the main thermocline on the time scales of decades, but only a small fraction of surface waters are mixed into the abyssal ocean on that time scale.

To predict the pace of climate change in response to the build-up of greenhouse gases in the atmosphere, we must learn to model this process of downward mixing. Hoffert et al. (1980), Cess and Goldenberg (1981) and Hansen et al. (1984) considered the ocean's role

in the transient response of climate to carbon dioxide forcing in terms of simple box models or one-dimensional models. Their work has been extended by Harvey and Schneider (1985) and Wigley and Schlesinger (1985). Sarmiento (1983) in a simulation of the tritium penetration of the North Atlantic has shown the importance of three-dimensional modeling to capture the actual processes which determine the fate of transient tracers. The fundamental problem with one-dimensional models is that they must be calibrated, and the calibration (Bacastrow and Bjorkstrom 1981) based on one transient tracer with a given input distribution over the World Ocean may not apply to another case with a different input. Bryan et al. (1982) is an attempt to examine the carbon dioxide climate response using a fully three-dimensional, coupled ocean–atmosphere model, in which the ocean has a very simple geometry. The results were analyzed in more detail in subsequent papers by Spelman and Manabe (1984) and Bryan and Spelman (1985). The same problem has also been studied by Schlesinger et al. (1985), using a coupled ocean–atmosphere model which has seasonal variation of insolation and realistic, global geography. The details of the ocean response in that study have recently been explored by Schlesinger and Jiang (1988). In contrast, the present study is a less ambitious extension of the earlier work of Bryan et al. (1982). Seasons are not included, the geometry of the oceans is still highly idealized, and cloud cover is specified. However, differences are allowed between the ocean circulation in two hemispheres, one of which is predominately ocean-covered and one of which is predominately land-covered. In addition sea surface salinity is freely predicted by the water balance of the model. The motivation is to clarify key processes in the ocean's role in climatic response to carbon dioxide warming rather than to attempt to include all relevant elements of the climate system.

The simple ocean–land geometry of Bryan et al. (1982) avoided some of the complexity of the real ocean. Only a single ocean basin in one hemisphere is considered. To provide a strong signal to noise ratio, the equilibrium climate was perturbed with a four-fold increase in atmospheric carbon dioxide. The ocean model causes a delay in climatic response to the new carbon dioxide level with an *e*-folding time of about two decades. The most significant result, however, was related to the pattern of the transient response of surface air temperature. About 25 years after the abrupt increase of the atmospheric concentration of carbon dioxide, the transient response of surface air temperature increases with latitude and is at a maximum near the pole. It qualitatively resembles the equilibrium response which can be attained after an infinite length of time. The effect of sea ice and polar halocline effectively insulates the atmosphere from the deep ocean and allows the large change of surface air temperature to take place near the pole.

Thompson and Schneider (1982) critically evaluated the study of Bryan et al. (1982). In their opinion the similarities between the transient and equilibrium temperature response patterns was attributable to the idealized geometry. They noted that the Southern Hemisphere, which is mostly covered by oceans, should have a very different response than the Northern Hemisphere. Although Thompson and Schneider (1982) used a very simple box model to illustrate their discussion, their conclusions appear to be reasonable and this study is an attempt to include a more realistic geometry. The new geometry is shown in Fig. 1. Only one basin is considered, but it extends over both hemispheres. The fractional coverage of the ocean at each latitude corresponds to that of the Earth's geography. Existing coupled models of the ocean and atmosphere have not been successful in simulating deep water formation in both the North Atlantic and near Antarctica at the same time. Rather than attempting to simulate the thermohaline circulation as observed, the present study tries to capture some of the important characteristics of the Northern and Southern hemisphere land–ocean distributions in a simpler context. In particular, it allows us to compare the climate response to rising atmospheric carbon dioxide in a predominately land-covered hemisphere to that in a predominately ocean-covered hemisphere.

2. The model structure

As noted in the Introduction, the coupled model is similar to that of Bryan et al. (1982) except for its geography as illustrated in Fig. 1. The domain consists of three identical sectors extending over both Northern and Southern hemispheres. The atmospheric component of the model is constrained to be periodic from one sector to another. Cyclic boundary conditions are also applied to the ocean in the narrow bands corresponding to the Drake Passage and Arctic Ocean where the ocean is continuous from one sector to another.

In the atmospheric component of the model the dynamic computation is performed using a spectral method in which the horizontal distributions of the predicted variables are represented by a limited number of spherical harmonics. The resolution is limited by a cutoff at a zonal wavenumber of 15. There is the same number of degrees of freedom in the meridional direction for each zonal wavenumber. The climate model contains a hydrologic cycle, including budgets of soil moisture and snow cover. To evaluate solar and terrestrial radiation, the effect of clouds, water vapor and ozone are taken into consideration. The distribution of water vapor is predicted in the model, but the mixing ratio of carbon dioxide is assumed to be a constant in the model atmosphere. Ozone is specified as a function of latitude and height from observations. The annually averaged values of height, thickness and fractional amount of cloud cover are also specified from data.

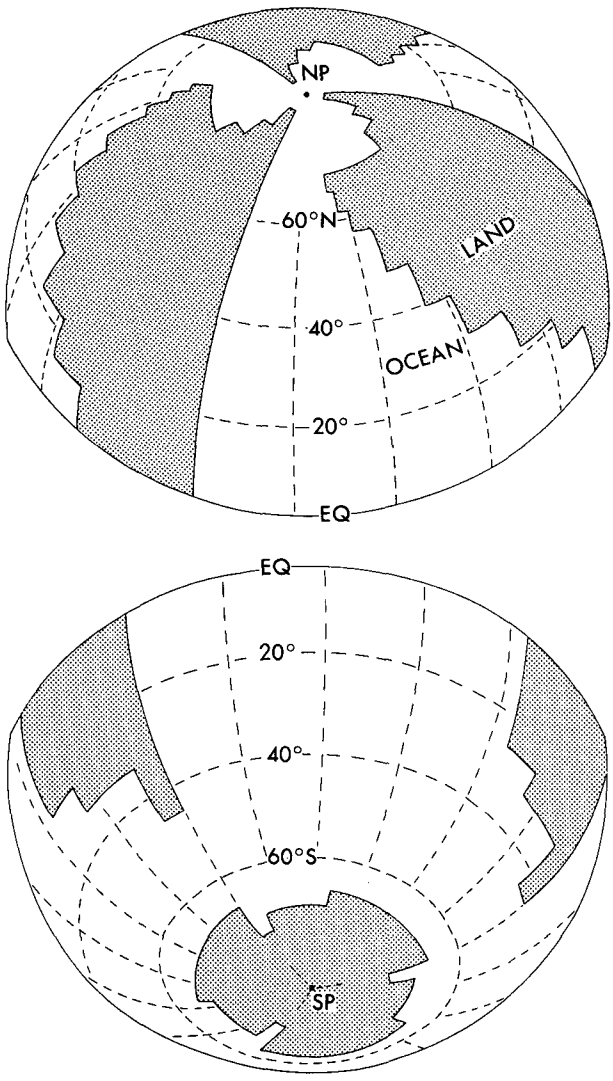

FIG. 1. Geometry of the coupled model. Cyclic boundary conditions are imposed along meridians 120° of longitude apart so that calculations only have to be carried out for one-third of the globe. The ratio of ocean to land at each latitude corresponds to the Earth's present geography. The ocean has a uniform depth of 5 km with the exception of the Drake Passage which is 3 km.

Another major simplification of the model is the specification of solar radiation without seasonal variations. The solar constant is taken as 1356 W m^{-2}. These simplifications are consistent with the goal of understanding the processes involved in a series of studies rather than attempting a single definitive calculation.

The temperature of the land surface is determined in such a way that it satisfies the assumption of no surface heat storage. That is, the contributions from net fluxes of solar and terrestrial radiations and turbulent fluxes of sensible and latent heat must balance locally. In this computation, zonally uniform albedo was specified as a function of latitude over the continents. However, it is replaced by higher local values when the surface is covered by snow.

The albedo of snow cover depends on surface temperature and snow depth. For deep snow (water equivalent at least 2 cm), the surface albedo is 60% if the surface temperature is below −10°C, and 45% at 0°C, with a linear interpolation between these values from −10° to 0°C. When the water equivalent of the snow depth is less than 2 cm, it is assumed that the albedo decreases from the deep snow values to the albedo of the underlying surface as a square root function of snow depth.

The oceanic component of the model is similar to the model of Bryan et al. (1975). The vertical computational resolution is enough to provide a description of the thermocline and the thermohaline circulation. The horizontal resolution of approximately 4.5° latitude by 3.8° longitude is only marginally adequate for resolving the intense coastal currents, and mesoscale eddies in the ocean are included only implicitly through lateral subgrid-scale mixing. The inclusion of salinity and a detailed equation of state for seawater allows for an interaction between the hydrological process in the atmosphere and the ocean circulation which is quite important in polar latitudes.

The prognostic system of sea ice is essentially similar to the very simple system developed by Bryan (1969). The sea ice is in free drift provided that its thickness is less than 4 m, but is stationary otherwise. The albedo of sea ice, which is necessary for the computation of the surface heat budget, depends on surface temperature and ice thickness. For thick sea ice (at least 1 m thick), the surface albedo is 80% if the surface temperature is below −10°C and 55% at 0°C, with a linear interpolation between these values from −10° to 0°C. If the ice thickness is less than 1 m, the albedo decreases from the thick ice values to the albedo of the underlying water surface as the square root of ice thickness. The freezing and thawing of sea ice interacts with the salinity field, but the effect is probably less important in this model than in the real ocean because of the lack of seasonal variations.

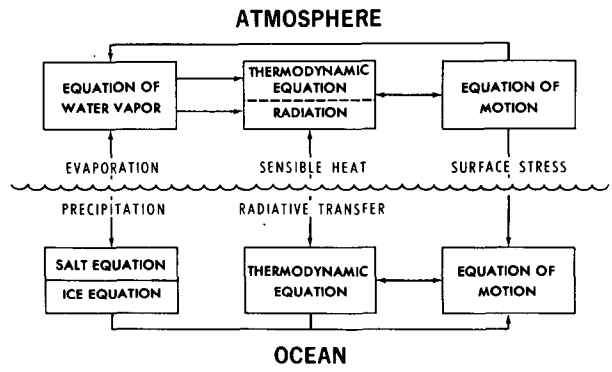

FIG. 2. Components of the coupled climate model.

The box diagram in Fig. 2 illustrates the major components of the coupled ocean–atmosphere model and the interaction among these components. The atmosphere and ocean of the coupled model interact with each other through exchanges of heat, water and momentum. Components of heat exchange are the net radiative flux and turbulent fluxes of sensible and latent heat. The components of water (or ice) exchange are evaporation (or sublimation), rainfall (or snowfall), and runoff from the continents. When the water equivalent of accumulated snow exceeds 20 cm, the excess snow is assumed to run off by glacial flow into the ocean. The rate of runoff is computed by assuming that the continental divide is a meridian located at the center of the model continent and that water flows in the zonal direction. However, the runoff from the polar continent in the Southern Hemisphere flows in the meridional direction. The ocean surface temperature and sea ice predicted in the ocean are used as the lower boundary condition for the atmosphere. Details of the heat, moisture and momentum exchange processes are given by Manabe (1969) and Manabe et al. (1975).

3. Equilibrium state

As pointed out in the Introduction, the heat capacity of the entire atmosphere is less than the heat capacity of the upper 3 m of the ocean. This explains why the thermal response-time to climate forcing of the atmosphere alone is relatively short, while the equilibration time of the coupled ocean–atmosphere system is of the order of centuries. Seeking climate equilibrium of a coupled ocean–atmosphere system through a direct numerical integration with respect to time is therefore impractical. Such an integration would have to resolve both the high frequencies related to synoptic systems in the atmosphere, and the ultralow frequencies related to the water mass adjustment in the deep ocean. As an alternative we seek a balanced thermal state through a relaxation procedure (Manabe and Bryan 1969; Bryan 1984). The atmosphere, the upper ocean, and the deep ocean are integrated with respect to time, using appropriate scales for each component. The time scales of the faster components are stretched so that the thermal response times of the "fast" and "slow" components become nearly equal. Boundary conditions consisting of the flow of heat, momentum and fresh water couple the "fast" and "slow" components of the model, and are updated at appropriate intervals. High frequency signals from boundary conditions generated by the atmosphere must be filtered out before they are applied to the "slow" ocean and sea-ice components of the model. In the present case the procedure is facilitated by the fact that seasonal variations are not considered. The atmospheric component of the model was numerically integrated over the equivalent of 8.2 years. At the same time the upper ocean was integrated over the equivalent of 1250 years, continuously exchanging boundary conditions with the overlying atmosphere. The length of integration in the deep ocean was 34 000 years. The adjustment is not perfect at the end of the asynchronous integration, but the residual drift in climate as measured by the change in the average sea surface temperature or the temperature averaged over the entire volume of the ocean appeared to be small enough to provide an adequate control for our response experiments. The details of the residual climate drift will be discussed in the next section.

A parallel computation was carried out to determine the equilibrium climate corresponding to twice the normal level of atmospheric carbon dioxide. The procedure for accelerating the convergence was identical. The difference between the two equilibrium climates provides a useful measure of the time-dependent response simulated by the coupled model.

The surface temperature and salinity patterns are critical for determining the thermohaline circulation in the ocean model and in determining the heat exchange between the ocean and atmosphere components. In Fig. 3 the model equilibrium surface patterns in the panels on the left may be compared with observations on the right. The latitude scale is the same for the panels on the right and the left, but the longitudinal scale of the model patterns is slightly expanded. Note that the model ocean is only 90 degrees of longitude wide at the equator, while the Pacific is about 150 degrees wide. For convenience we will refer to the hemisphere with the preponderance of land as the Northern Hemisphere and the largely ocean hemisphere as the Southern Hemisphere. The model surface temperature and salinity patterns resemble the observed patterns of the North Pacific rather than those of the North Atlantic. Figure 4b shows the meridional circulation in the model. Deep sinking is confined to polar and subpolar latitudes of the Southern Hemisphere. There is nothing corresponding to the formation of North Atlantic deep water in the Northern Hemisphere of the model. Observations indicate that intermediate water, but no deep water, is formed in the North Pacific. Thus there is a rationale for comparing the Northern Hemisphere ocean of the model with the North Pacific. The model obviously lacks anything equivalent to the deep water formation that is observed to take place in the North Atlantic. This missing feature could obviously bias the transient response of the coupled model, and we will return to this point in the final discussion in section 5.

There is a resemblance of the configuration of the 28° isotherm in the temperature pattern predicted by the model and observations in the Western Pacific. The simulation is not as good along the equator in the east. The model indicates high temperatures right at the eastern boundary and observations indicate relatively low temperatures along the coast of South America. There are relatively low temperatures off the coast of California associated with upwelling, and the model also shows relatively low temperatures in the corresponding location. In the Southern Hemisphere of the

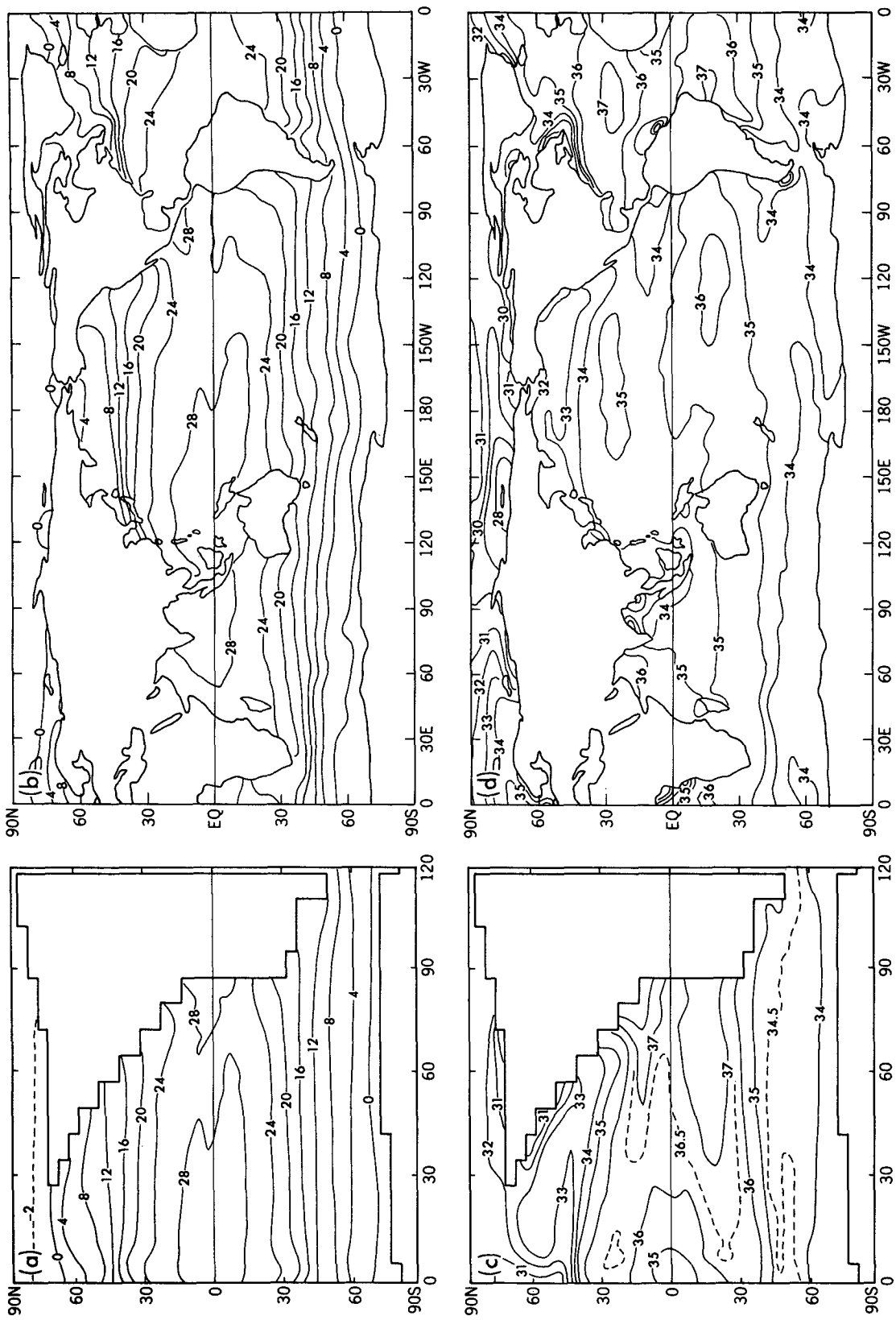

FIG. 3. (a) Sea surface temperature corresponding to the initial equilibrium for normal atmospheric carbon dioxide content. Units are degrees Centigrade. (b) Annual average of sea surface temperature as observed (Levitus 1982). (c) Same as (a) for model surface salinity. Units are parts per thousand. (d) Same as (b) for observed salinity.

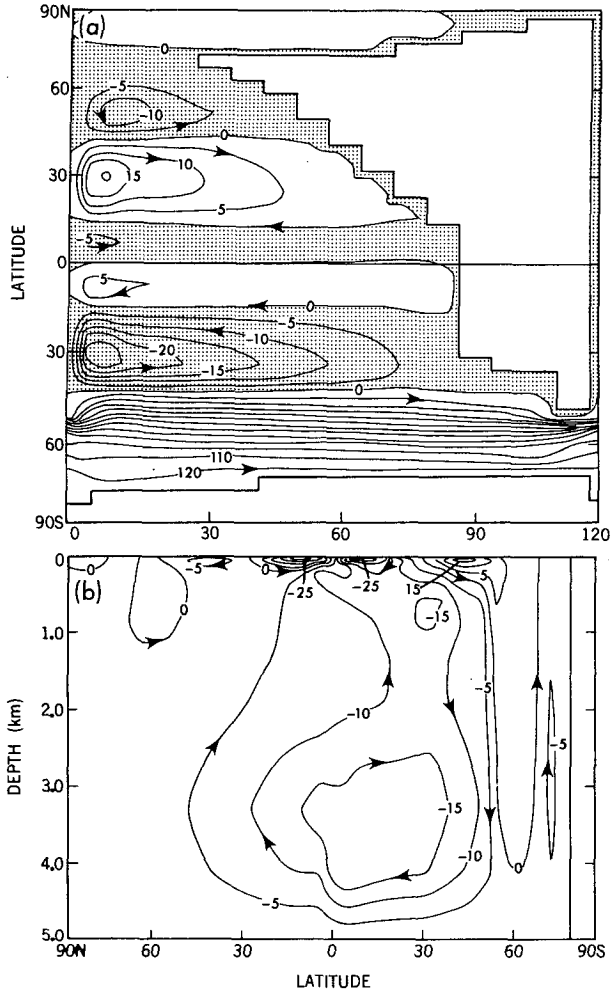

FIG. 4. (a) Streamfunction of the vertically integrated mass transport corresponding to the initial equilibrium climate for normal atmospheric carbon dioxide. (b) Streamfunction of the zonally integrated mass transport showing the meridional circulation of the ocean model. Units are in megatons per second.

model the sea surface temperatures are slightly higher than observed. Note that the 8°C isotherm goes right through the model Drake Passage, but in reality only the 4° and 0° isotherms go through.

The model simulates the distinctive tongue of fresh surface water along the eastern boundary in the North Pacific. In the tropical and subtropical latitudes, however, the surface salinity is much higher in the model than in the Pacific. The values are much closer to those found in the Atlantic. The geometry of the model may be an important factor. In the Pacific there is a flow through the Indonesian Archipelago which carries equatorial surface waters into the Indian Ocean. Since the model is closed on the western equatorial boundary, the large region of low surface salinity in that area may be thought of as corresponding to the low surface salinities in the Eastern Indian Ocean. In the Eastern Equatorial Pacific trade winds either flow over the narrow Isthmus of Panama or are blocked by the Andes Mountains. In the model the trade winds have a long trajectory over land before moving over the ocean. The situation in the model in this respect is much more like the Atlantic than the Pacific. The relatively high surface salinities in the model are more like those found in the Atlantic than the Pacific.

A mass transport streamfunction may be defined as

$$\partial_y\psi,\ \partial_x\psi = \int_{-H}^{0} \rho(-u,\ v)dz. \qquad (3.1)$$

The pattern of flow corresponding to the initial climate equilibrium is shown in Fig. 4a. In the Northern Hemisphere of the model the dominant feature is a clockwise subtropical gyre centered at 30 N with a strength of about 20 Mt s^{-1}. Because the oceans narrows to the north, the subarctic gyre occupies a much smaller area and is correspondingly weaker. In the Southern Hemisphere of the model there is a subtropical gyre corresponding to the one in the Northern Hemisphere, but the principal feature is a circumpolar current with a total transport of 120 Mt s^{-1}. By way of comparison, measurements in the Drake Passage for one year (Whitworth 1983) indicated that the transport varied from 118–146 Mt s^{-1}.

A very different perspective on the circulation in the model ocean is given by the zonally integrated overturning in the meridional plane. Let

$$\partial_z\psi,\ \partial_y\psi = \int_0^{\lambda'} \rho(-v,\ w)\cos\phi a d\lambda. \qquad (3.2)$$

The pattern of meridional circulation shown in Fig. 4b consists of sinking in the Southern Hemisphere and rising motion in the Northern Hemisphere. The Northern Hemisphere ocean of the model corresponds to the North Pacific. Near the surface in both hemispheres the meridional circulation of the model is dominated by Ekman transport in the planetary boundary layer. In the trade wind zone the Ekman transport is poleward in both hemispheres, causing a concentrated upwelling at the equator. In the vicinity of the westerlies the Ekman transport is equatorward. In the Northern Hemisphere the Ekman flow under the westerlies is compensated by a shallow return flow in the upper thermocline. In the Southern Hemisphere, on the other hand, the Ekman flow under the westerlies is compensated by a very deep cell extending well below the main thermocline. The existence of deep downwelling equatorward of the Circumpolar Current and deep upwelling south of the current was originally suggested by Deacon (1937) on the basis of the results of the *Challenger* Expedition. The dynamics of this circulation are explored in the numerical experiments of Gill and Bryan (1971). In order to provide insight we have calculated the equilibrium climate and ocean circulation for a case which is identical to the reference normal carbon dioxide case, except that the gap

through the Drake Passage is closed off. The meridional circulation corresponding to the closed gap case is shown in Fig. 5. Again the sinking is largely confined to the Southern Hemisphere, but the pattern is very different. A single downward branch exists in the vicinity of the southern boundary. There is no deep wind-driven cell in the ocean below the Southern Hemisphere westerlies.

Gill and Bryan (1971) explain the deep cell in the open gap case as the result of the constraint imposed by the Earth's rotation. Zonally averaged meridional flow can be geostrophically balanced when the ocean basin is confined between walls on the eastern and western boundaries. In the latitude of the gap other terms in the momentum equations must balance the Coriolis term associated with meridional motion. Since inertial effects are relatively small in the model (and in the real ocean) nongeostrophic meridional flow below the Ekman layer is very weak in the gap. Thus the wind induced equatorward flow under the Southern Hemisphere westerlies can only be compensated by a deep downwelling north of the gap, southward geostrophic flow at the base of the gap, and deep upwelling south of the Circumpolar Current. Recently the picture of the meridional circulation presented by Deacon has been extended by McCartney (1977). In a more detailed analysis of water mass data McCartney points out that the downwelling north of the gap is probably very concentrated at certain longitudes. In particular the ocean off the coast of Southern Chile may be the most important downward pathway. This finding is consistent with vertical motion patterns in the numerical experiments of Gill and Bryan (1971) and the present model.

Zonally averaged temperatures in the coupled model may be compared to observations in the Pacific in Fig. 6. The temperature structure of the atmosphere is reasonably well simulated, but the model ocean thermocline tends to be too thick, and deep water too warm. Cold dense waters formed near the surface in polar ocean areas of the model tend to entrain unrealistic amounts of surrounding water as they move downward in a model of limited horizontal resolution. Thus it is difficult to get realistic deep water properties.

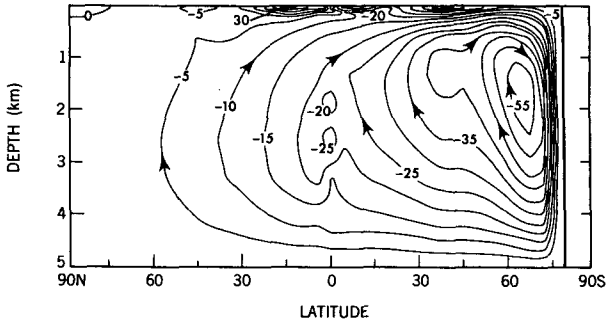

FIG. 5. The zonally integrated flow corresponding to an equilibrium climate for the normal atmospheric carbon dioxide case except that the gap corresponding to the Drake Passage is closed. The pattern may be compared to Fig. 46. Units are megatons per second.

The same difficulty is apparent in the simulation of the salinity field shown in Fig. 7. The model is unable to reproduce the tongues of intermediate, low salinity water of the Pacific which are formed in subarctic areas and push equatorward at the base of the main thermocline. Halocline regions are formed in the polar oceans as observed, but the high salinity waters formed at the surface in the subtropics spread out to form an unrealistic deep lens within the main thermocline of the model ocean.

4. Transient response

a. Temperature change at the surface

The previous section describes the solution obtained by an extended asynchronous experiment with distorted time scales applied to the "fast" and "slow" components of the climate model. This solution was tested in a control run by carrying out an extended integration with no distortion of the thermal time scales of the atmosphere and ocean. Only in the ocean model was the dynamic distortion retained to slow down the speed of internal gravity waves (Bryan 1984). The average sea surface temperature is plotted as a function of time in Fig. 8. After about 30 years of integration, the average sea surface temperature leveled out at about 17.8°C for the remaining 80 years of the integration. During the entire integration the volume-averaged temperature rose steadily, indicating a net heating of the ocean equivalent to a downward flux at the surface of approximately 0.6 W m^{-2}. This is a measure of lack of equilibrium in the initial climate obtained by asynchronous integration. A flux of heat of 1 W m^{-2} would be less than the error of heat balance calculations with conventional air–sea data. Nevertheless, a smaller drift would be desirable, since the net heating associated with a doubling of atmospheric carbon dioxide is only about 2.5 W m^{-2}.

The curves labeled A, B and C in Fig. 8 represent three "switch on" experiments in which atmospheric carbon dioxide is doubled at the start of each run. The ordinate is the globally averaged sea surface temperature. Note that variability with respect to time causes significant differences in response, clearly indicating the need for an ensemble of experiments to obtain a more reliable average response. The response is isolated in Fig. 9a by subtracting the control run temperatures from curves A, B and C. The heavy solid line is the average of the individual experiments. The response was characterized by a sudden rise in less than 5 years to a level of approximately 0.25. This was followed by a slow steady rise over the next four decades to a final value of about 0.5 after 50 years. The *e*-folding time for the global mean temperature response is quite similar to that obtained by Schlesinger et al. (1985), but

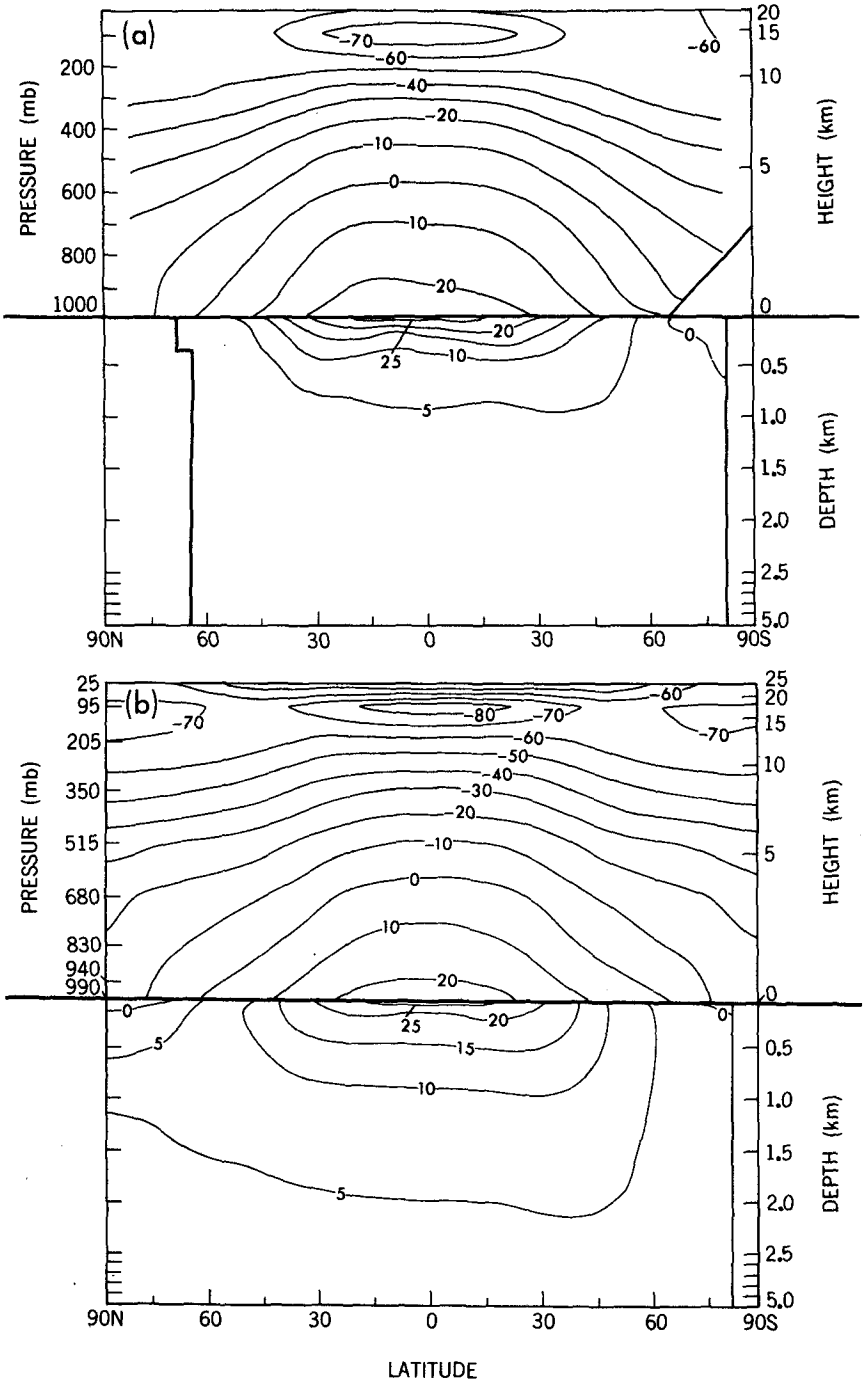

FIG. 6. (a) Observed zonally averaged and annually averaged temperatures in the ocean and atmosphere. Units are degrees Centigrade. Atmospheric data from Oort (1983). Ocean data from Levitus (1982) for the Pacific. (b) Computed temperatures from the initial climate for the coupled model.

the details of the coupled models are so different that the correspondence may not be very significant. The ensemble-average response for the Northern and Southern hemispheres of the model are shown separately in Fig. 9b. All subsequent figures will also refer to the ensemble-average transient response. A very different response in sea surface temperature is indicated for the Northern Hemisphere, which is covered by large land masses, and the Southern Hemisphere, which is oceanic over most of the total surface area. In the

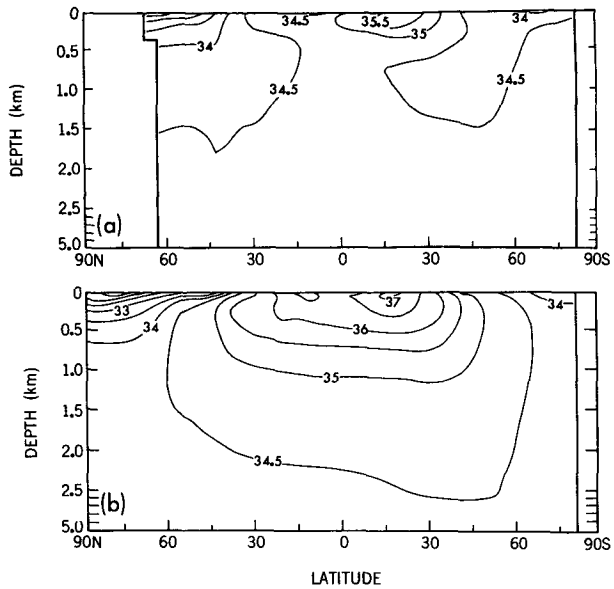

FIG. 7. (a) Observed zonally averaged and annually averaged salinity for the Pacific in parts per thousand. (b) Computed salinity for the initial climate equilibrium.

northern land-hemisphere a response of about 0.6 is reached within one decade after "switch on" followed by a slow rise of about 0.04 per decade. In the southern ocean-hemisphere an initial response of about 0.15 is followed by a steady rise of about 0.04 per decade. The difference between the response in the two hemispheres is striking, and very consistent with the conjecture of Thompson and Schneider (1982) discussed in the Introduction. As will be shown later, however, the differences in response between the hemispheres are too large to be accounted for solely by the simple mechanism they propose.

More insight on the latitudinal dependence of the response may be gained from Fig. 10, which shows the normalized response of zonally averaged sea surface temperature as a function of latitude and time after "switch on" for the ensemble of experiments. The Northern Hemisphere of the model indicated a rather uniform response with respect to latitude from the equator to 60°N. At higher latitudes the ocean was covered with sea ice which retreats very slowly and forces the sea surface temperatures to remain at the freezing point. In general, the sea surface temperature of the Southern Hemisphere responded at a slower pace than that of the Northern Hemisphere. In the immediate vicinity of the southern continent, it hardly changed at all. There was a large variability in polar latitudes which is greatest in the vicinity of the boundary of the polar ice pack.

The analysis of air temperatures near the ground allows the possibility of comparing the response over land to the response over the ocean. In Fig. 11 we have the zonally averaged normalized response of air temperatures as a function of time after "switch on". In general, air temperatures over the sea compare closely with sea surface temperatures. A notable exception occurs over sea ice, which serves as a thermal insulation between the atmosphere and underlying sea water. In Northern Hemisphere polar regions the normalized response of surface air temperature is up to 0.5 over the ice, compared to no response for sea surface temperature in Fig. 10. The thermal insulation effect of sea ice identified here helps maintain the latitudinal uniformity in the normalized response of surface air temperature despite the absence of sea surface warming

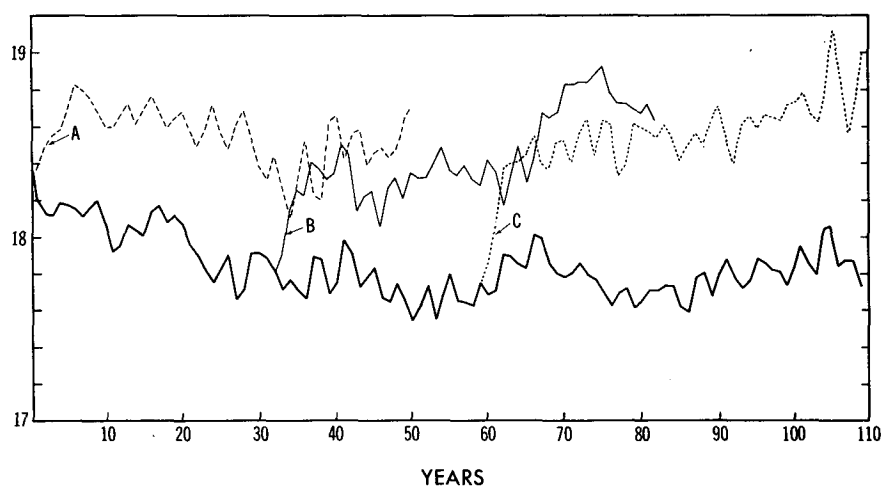

FIG. 8. Globally averaged sea surface temperature (degrees Centigrade) of the model as a function of time during the synchronous integration in which the thermal time scales of all components of the climate model are kept the same. The thick line corresponds to the control run with fixed normal atmospheric carbon dioxide. The thin curves A, B and C represent "switch on" experiments in which the atmospheric carbon dioxide is doubled.

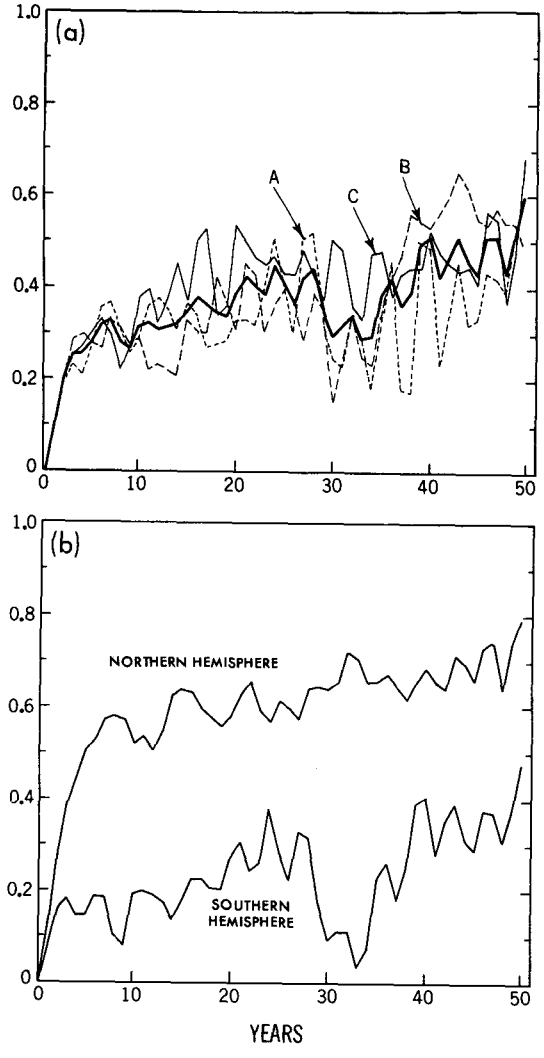

FIG. 9. The transient response of the area-averaged annual mean sea surface temperature normalized by the equilibrium response as a function of time after "switch on". (a) The globally averaged response for the ensemble of experiments. (b) The ensemble averages for the Northern and Southern hemisphere ocean are shown separately.

in these regions. The patterns of air temperature response over both the land and sea confirm the impression of Fig. 9 that the major changes took place in the first decade after "switch on" and further changes were extremely slow. The most obvious trends are in the air temperatures over the Southern Hemisphere Ocean where the 0.5 response line moved slowly from about 20° to 40°S from year 10 to year 50. The most striking feature of the response of air temperature over land surfaces was the *uniformity of the normalized response* from the Northern Hemisphere of the model right down to 30°S. The uniform normalized response with respect to latitude does not imply that the actual temperature rise is uniform, only that the pattern of zonal mean response is similar to the equilibrium-response. As Thompson and Schneider (1982) predicted, the response is very different in the Southern Hemisphere where most of the surface is covered by ocean. However, the surface air temperature over land surfaces in low latitudes of the Southern Hemisphere appeared to change in concert with the Northern Hemisphere in spite of the lag in the response of the Southern sea surface temperature.

b. Response above and below the surface

Up to this point the "switch on" solutions of the coupled model have been examined only in terms of temperature adjacent to the surface of the ocean and land. To provide an understanding of the processes involved, it is necessary to look at the response in three dimensions. Fig. 12a shows the zonally averaged temperature difference between equilibrium climates for twice normal and normal atmospheric carbon dioxide. The ordinate scale is chosen to provide detail in the lower atmosphere and the upper ocean. The main features of the response pattern are similar to the coupled ocean–atmosphere study with a single hemisphere (Spelman and Manabe 1984). In the atmosphere the maximum warming appears in the stable surface layer over the pole and is associated with the positive feedback effect of snow cover and sea ice. The warming is relatively large in the upper troposphere over the equator. In the lower stratosphere there is a slight cooling. Note that the equilibrium response is nearly symmetrical across the equator.

The strong polar amplification shown in Fig. 12a is consistent with earlier sensitivity studies (Manabe and Wetherald 1975). The uniformity of the normalized response with respect to latitude shown in Fig. 11 shows that over land areas in the Northern Hemisphere the transient response is also polar amplified. A similar conclusion was made by Bryan et al. (1982) and Spelman and Manabe (1984) on the basis of a one hemisphere model. As we have already noted, it does not hold up at all for surface air temperature in the Southern Hemisphere.

In the ocean the equilibrium response is greater in the deep ocean than it is at the surface for most latitudes. As pointed out by Spelman and Manabe (1984) and Manabe and Bryan (1985), this is simply due to the fact that deep waters of the ocean are formed at high latitudes where polar amplification leads to greater climate sensitivity. Figure 12b is the transient response averaged over the period from 41–50 years after "switch on". If one compares this figure with the equilibrium response, one finds the largest difference in the deep ocean waters. On a 40-to-50 year time scale most of the transient temperature response was still confined to the upper ocean and only penetrated to greater depths in the zone of active deep water formation in the Southern Hemisphere polar region. In the upper thermocline the warming is particularly large around

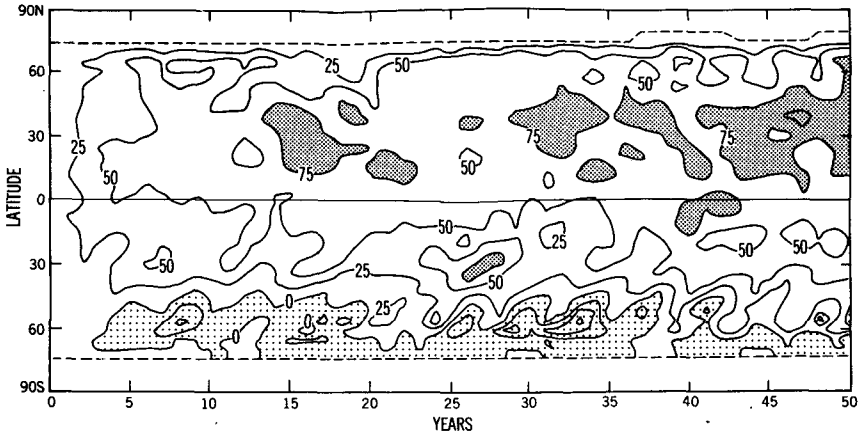

FIG. 10. Zonally averaged normalized response of sea surface temperature shown as a function of latitude and time. Dashed line indicates the boundary of polar pack ice. Units are percent of total equilibrium response.

50°–60°N in the Northern Hemisphere. In the polar region of the Northern Hemisphere the warming of the model ocean is very weak, but the warming of the overlying air is very pronounced. Both sea ice and the polar halocline tend to decouple the atmosphere from the deep ocean allowing polar amplification of atmospheric warming to take place in the Northern Hemisphere. In the Southern Hemisphere the thermal anomaly penetrated deeply, but the amplitude was very small as indicated by the analysis of sea surface tem-

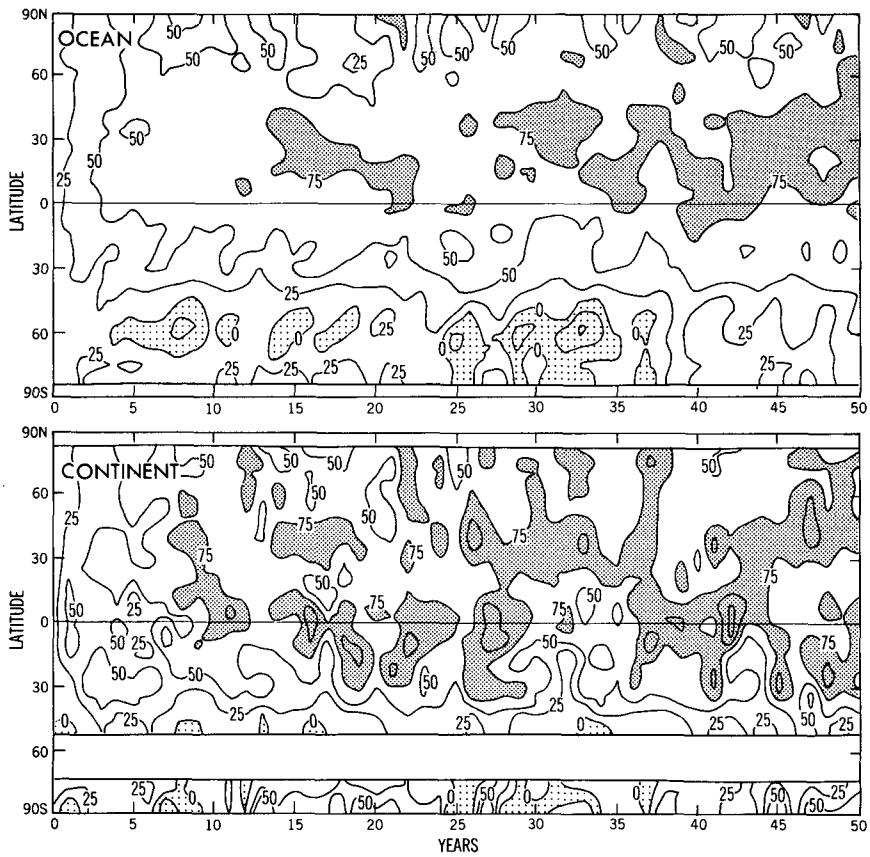

FIG. 11. As in Fig. 10, but for surface air temperature.

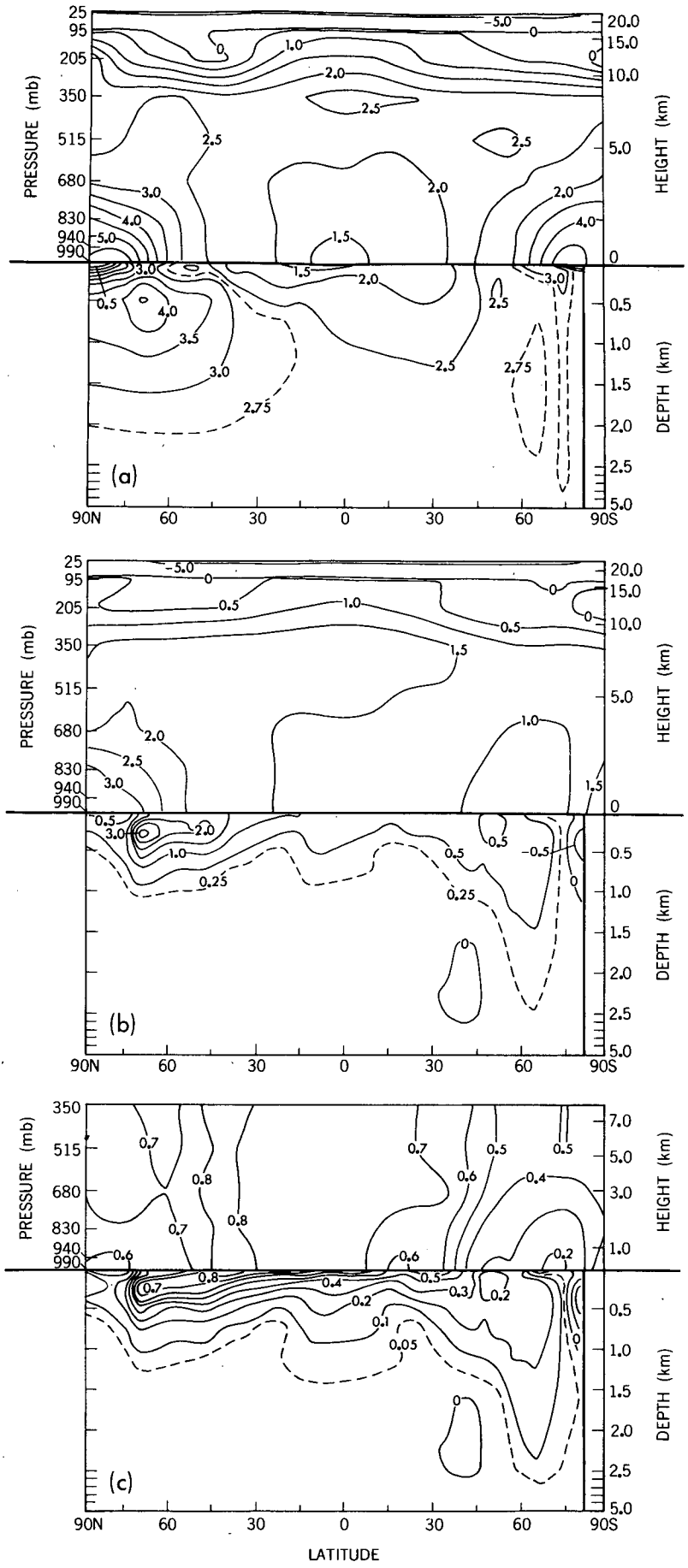
PRESSURE (mb)
HEIGHT (km)
DEPTH (km)
(a)
(b)
(c)
90N
60
30
0
30
60
90S
LATITUDE

perature response. The atmosphere indicates a marked asymmetry between the hemispheres in the transient response in Fig. 12b.

It should be noted, however, that there is no equivalent of North Atlantic Deep Water formation in the present model. This undoubtedly speeds up the climatic response in the Northern Hemisphere relative to a more realistic model. We will return to this point in the final section. The interesting new feature was the very small oceanic response in the high latitudes of the Southern Hemisphere, associated with the great expanse of ocean and deep penetration of the heat anomaly in the vicinity of the Circumpolar Current. Note that in the vicinity of the southern polar land boundary the ocean has actually cooled by 0.5°C. We will return to this result in the final discussion.

The normalized response shown in Fig. 12c is simply the transient response shown in Fig. 12b divided by the equilibrium response shown in Fig. 12a. Note that in the atmosphere the high normalized response in the Northern Hemisphere was fairly uniform within the troposphere. In the Southern Hemisphere, however, the layer of small response was confined to a region close to the surface in high latitudes. In the ocean the high normalized response region in the Northern Hemisphere penetrates poleward below the stable halocline near the pole. The halocline acted as a barrier to the downward penetration of surface influences. This effect might be modified somewhat if seasons were included in the model.

To provide a background for understanding the very deep penetration of the thermal anomaly in the Southern Hemisphere, the zonally integrated overturning is shown in Fig. 13. The patterns represent an average for the years 41–50 after "switch on". Changes in the meridional circulation can be seen by comparing Fig. 13 with Fig. 4b. From the standpoint of response in the Southern Hemisphere the important point is that the deep circulation, downward on the equatorward side of the gap and upward on the poleward side, was still present. The downward flow on one side of the gap provided an important downward pathway and the upward flow continued to supply deep water to the surface which was untouched by the "switch on" event.

The gradual build up of the oceanic heat storage with respect to time is shown in the two panels of Fig. 14. The zonally averaged increase in heat storage per unit area is plotted in the upper panel. As shown in Fig. 12b the penetration of heat is very shallow, but intense in the Northern Hemisphere. In the Southern Hemisphere the penetration is much deeper, but the strength of the anomaly is much weaker. The result is

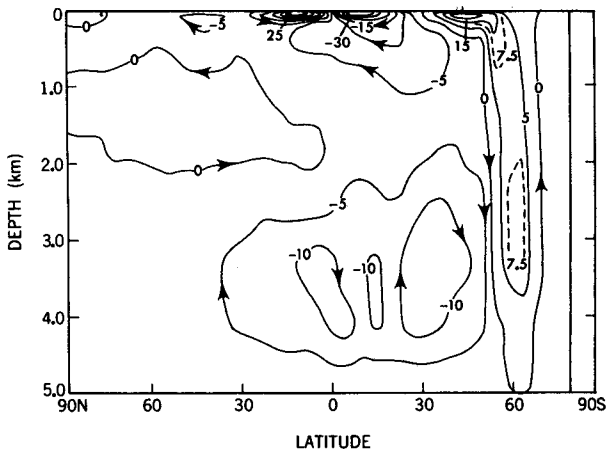

FIG. 13. The zonally integrated mass transport in units of megatons per second averaged over the 41–50 years after "switch on".

almost perfect compensation and the heat storage per unit area is quite symmetric across the equator.

The lower panel of Fig. 14 shows the total zonally integrated heat storage. In this case the width of the ocean becomes important. In the Northern Hemisphere the maximum heat storage occurs at midlatitudes rather than at subpolar latitudes because the area of ocean shrinks so rapidly with increasing latitude. The dominance of the Southern Ocean with its huge area is obvious. In the first 5 years after "switch on" the total heat stored at each latitude is nearly symmetrical across the equator indicating that the CO_2 heating of the two hemispheres is similar. After this initial period, the zonally integrated storage of heat in the Southern Hemisphere becomes significantly larger than the heat storage in the Northern Hemisphere. This is because the sea surface temperature fails to increase in high latitudes of the Southern Hemisphere as described earlier, thereby lowering the surface cooling due to evaporation and sensible heat transfer. In summary, it is clear that the geography of the Southern Ocean of the model and the deep sinking and upwelling near the Drake Passage allow the Southern Hemisphere Ocean to be a very effective brake on climate change due to external forcing.

c. Heat balance of the Southern Ocean

The previous discussion provides a qualitative picture of the thermal response. The purpose of this section is to present a more quantitative analysis of the mechanisms involved. The local heat balance of the ocean may be represented as

FIG. 12. Zonally averaged temperature response of the model. (a) Equilibrium response. Units are ° Centigrade. (b) Transient response averaged over the period 41–50 years after "switch on". (c) Normalized response corresponding to (b) divided by (a).

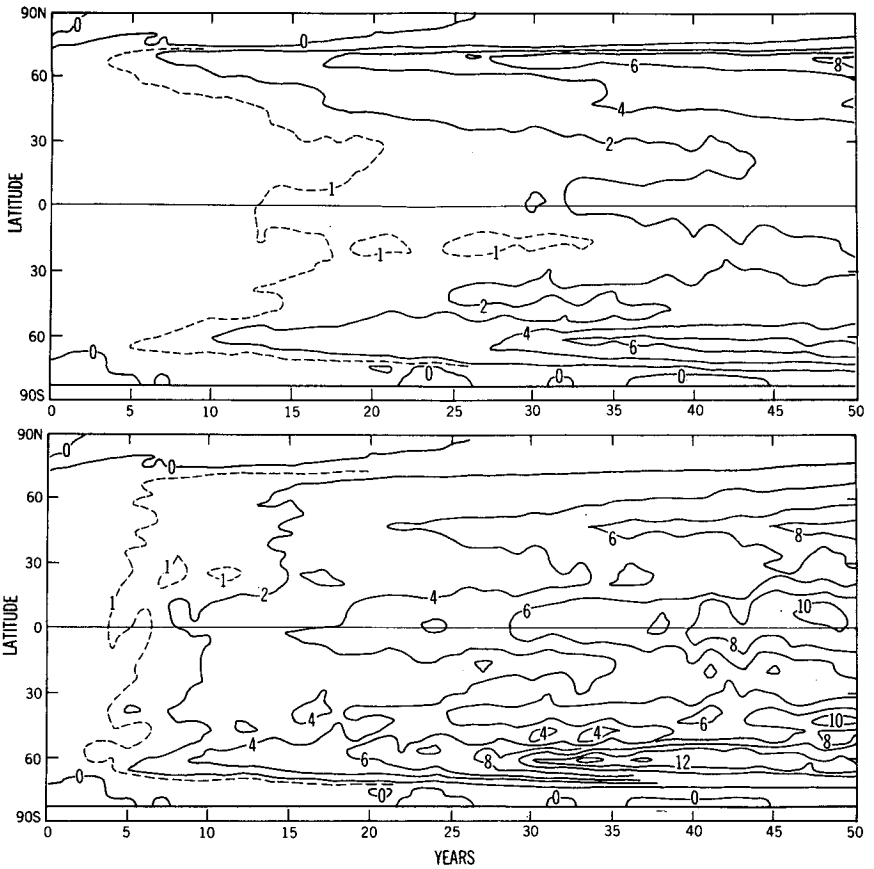

FIG. 14. (Upper panel) The average of excess heat content in the water column per unit area as a function of time. Units are 10^9 J m^{-2}. (Lower panel) Total heat storage for an entire 1° latitude belt in units of 10^{21} J.

$$\partial_t T = \text{Advection} + \text{Horizontal diffusion} + \text{Convection}. \quad (4.1)$$

In this breakdown of the heat balance vertical and horizontal advection are combined, and subgrid-scale vertical mixing is lumped together with convection. Horizontal diffusion is the contribution from the subgrid-scale, horizontal mixing.

The zonally averaged values of these terms in the upper 500 m layer of the model ocean are shown in Fig. 15 for the interval from 46° to 90°S. This interval covers both the subpolar and polar regions of the Southern Hemisphere. The heat balance is taken over the period 16–35 years after "switch on". The average for the control run is shown in Fig. 15a. Through most of the water column lateral diffusion and advection caused warming. This was associated with a convergence of warm waters into the subpolar and polar areas. The cooling effect of advection in the mixed layer can be understood in terms of the meridional circulation (Fig. 4b) and temperature field (Fig. 5b). The Ekman transport under the westerlies is equatorward and it sweeps cold polar waters with it. The Ekman flux is kinematically compensated at deeper levels by slightly warmer waters moving poleward. Convection in the ocean normally transports heat upward, warming the surface and cooling lower levels.

The heat balance for the control run subtracted from the heat balance in the "switch on" case is shown in Fig. 15b. The convection below the surface is slightly stronger in the "switch on" case, but it is compensated by stronger equatorward Ekman transport associated with an increase in zonal winds. Stronger westerlies appear to be due to the increased poleward temperature gradient associated with higher sea surface temperatures in lower latitudes of the Southern Ocean and almost no change in sea surface temperature at high latitudes. Below the surface level the change in the heat balance is much smaller. The analysis described above clearly indicates that the equatorward advection of upwelled cold water by the Ekman drift currents prevents the net warming of the sea surface despite the warming tendency due to increased vertical mixing near the surface.

Next we examine the heat balance in a narrower zone centered on the Circumpolar Current where the downward penetration of the warm anomaly is most pronounced. This analysis is shown in Fig. 16. In this

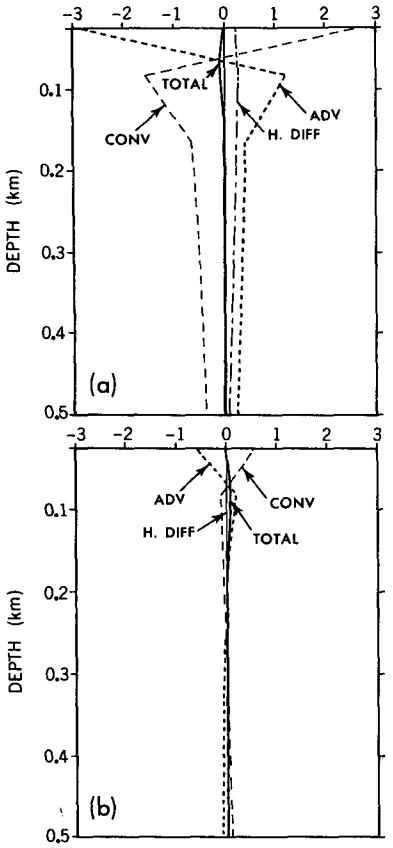

FIG. 15. Components of the heat balance defined in (4.1) averaged over the entire ocean area from 46°S to 90°S. (a) Corresponding to the control run. Units are 10^{-8} °C s^{-1}. (b) The difference between the control run and "switch on" averaged over the years 16–35.

case we consider the water column down to 3 km, but the breakdown is the same as in the previous figure. In the control case shown in Fig. 16a advection and horizontal diffusion caused warming throughout the water column. Both terms supply heat to this region from lower latitudes. Convection and vertical diffusion acted to cool the deep water column by transporting heat to the surface where it was transferred to the atmosphere. The effect of the warming event shown in Fig. 16b was to weaken both advection and convection in most of the water column with the exception of the surface layer. In other words, the convergence of heat transport into this zone became less and the upward transport of heat became less. However, the weakening of convection was greater, so that the net effect was an accumulation of heat below the surface that extended to great depths in the vicinity of the Circumpolar Current.

5. Summary and conclusions

A coupled model of the ocean and atmosphere is a new tool for climate research which builds on the success achieved with atmospheric models. It is particularly appropriate for studying the response of climate to an externally imposed change of carbon dioxide, since the ocean plays an important role in controlling the time scales of climate change. The present study is a continuation of the previous transient climate calculations analyzed by Bryan et al. (1982), Spelman and Manabe (1984) and Bryan and Spelman (1985). The new factor introduced is a much more general geometry which provides for an asymmetric response between hemispheres and a simulation of the main features of the Southern Ocean. No attempt has been made to include the carbon cycle and the interaction of climate and the biosphere. Our calculations are restricted to the response of a coupled atmosphere–ocean model to specified changes in atmospheric carbon dioxide.

A very different response was found in the predominantly land-covered Northern Hemisphere compared to the largely ocean-covered Southern Hemisphere. In the predominantly ocean-covered hemisphere the re-

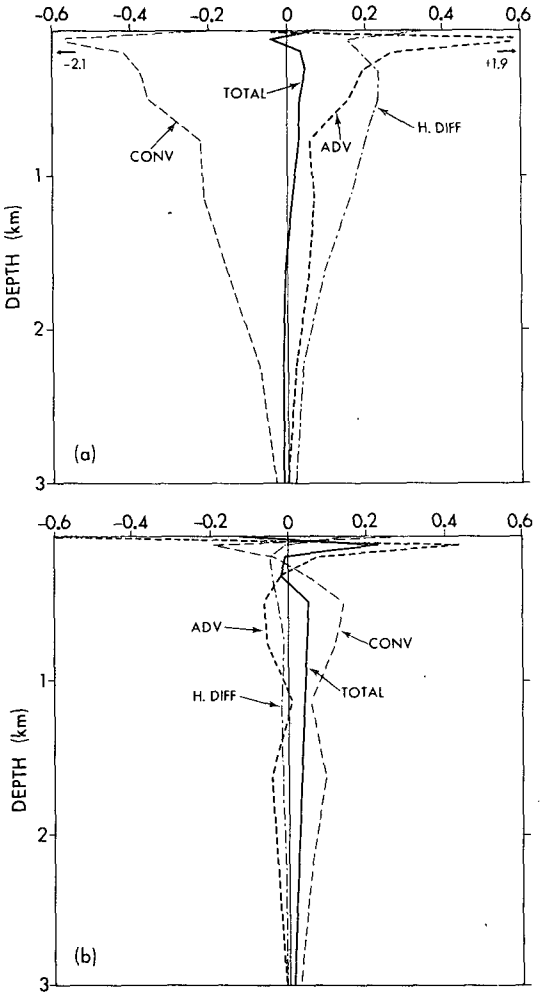

FIG. 16. As in Fig. 15 averaged over the more limited zonal belt between 55° and 64°S.

sponse of sea surface temperature lags substantially behind the corresponding response in the predominantly land-covered hemisphere. This is consistent with the prediction of Thompson and Schneider (1982) mentioned in the Introduction. However, it is of particular interest that there was almost no response in polar latitudes of the Southern Ocean four decades after "switch on". In fact there was a slight cooling poleward of the Circumpolar Current. The analysis of the heat balance suggests that this is not just due to the large extent of ocean. In the presence of a Circumpolar Current the response of the ocean is fundamentally different. Dynamic constraints (Gill and Bryan 1971) force a deep downwelling equatorward of the Circumpolar Current and a deep upwelling poleward of the current. The low response at very high latitudes is in part due to the fact that the surface of the ocean is being continually renewed by virgin waters from great depth.

The minimum response in the polar region of the Southern Hemisphere of the model has wide implications. It has frequently been suggested that warming of the seas around Antarctica and a possible destabilization of the Antarctic ice cap could lead to a drastic rise in global sea level. The present study suggests even if such an instability were possible, the precondition of warming in the seas around Antarctica may not occur for a long time after warming has already taken place in the lower latitudes of the Southern Hemisphere and in the Northern Hemisphere. In our previous study (Bryan et al. 1982) it was concluded that the response pattern of zonal mean surface air temperature to a slow carbon-dioxide warming would be qualitatively similar to that for equilibrium response. The present study shows that this is true only for the Northern Hemisphere. The geometry of the present model is very unlike that of the actual continent–ocean distribution. A question might arise as to the applicability of the results in a more realistic context. Currently a similar response experiment is being carried out in a model with more realistic geometry and preliminary results confirm the lack of response and even of a slight cooling of sea surface temperatures in the high latitude Southern Ocean.

In the Weddell Sea there is a time series of deep-sea temperature measurements that goes back to the early part of the century. While the long term trend in sea surface measurements appears to be nearly constant or slightly upward in the Southern Hemisphere (Jones et al. 1986), the trend in deep Weddell Sea temperatures is downward (Gordon 1982). In the light of the response of ocean temperatures indicated in our numerical experiments, opposite trends in surface waters at lower latitudes in the Southern Hemisphere and deep waters around the Antarctic Continent are not implausible.

A caveat naturally arises in the physical interpretation of our results because there is no deep water formation in the Northern Hemisphere of the model equivalent to the formation of North Atlantic Deep Water. However, new calculations have recently been completed which include the actual geometry of the World Ocean and realistic deep water production in the Northern Hemisphere. The same asymmetry in the transient response between the hemispheres is found, suggesting that the results of the present study are quite robust.

A key feature in producing the asymmetry between the hemispheres is a deep meridional cell in the vicinity of the circumpolar current. Would this cell exist if seasonal variations were included in the model? A positive indication is provided by the results of a previous study by Bryan and Lewis (1979). In a World Ocean model driven by seasonally varying, observed boundary conditions at the ocean surface, a deep meridional circulation exists, which is very similar to the meridional cell in the vicinity of the circumpolar current in the present model.

At this stage coupled models of the ocean and atmosphere are designed to investigate the feedback mechanisms in climate. For this purpose deliberate simplifications are useful. Due to the very simplified geometry of the ocean model used in the present study, the lack of seasonal variations and predicted cloudiness, it is not possible to make a quantitative comparison with the results obtained by Schlesinger et al. (1985). The main qualitative difference is that the present model appears to support a marked asymmetry in the response of the Northern and Southern hemispheres as predicted by Thompson and Schneider (1982), while the Schlesinger et al. (1985) results show only a very weak asymmetry. Further numerical experiments will be needed to clarify this difference. As the important feedbacks of the climate system become more clearly defined, it will be appropriate to refine the models and attempt calculations that are increasingly more accurate simulations.

Hansen et al. (1984) noted that the interaction between cloud cover and radiation may have a positive feedback effect which delays the response of a coupled model to a thermal forcing. Therefore, it is urgent to improve the parameterization of this feedback process and incorporate it into the model in order to obtain a better estimate of the transient response of climate. Other obvious improvements are to include the effect of seasons and realistic geometry of the oceans. Increased resolution of both atmospheric and oceanic components of the model would allow a much more realistic representation of variability. In the long run a prediction of changes in climate variability over the globe may be as important as predicting changes in time-averaged quantities.

Acknowledgments. We wish to thank R. Stouffer and K. Dixon for their assistance in the modeling and analysis of the coupled ocean–atmosphere model. The constructive comments of I. Held and C. Boening were very helpful for improving the manuscript. We

gratefully acknowledge GFDL staff members P. Tunison and J. Connor for their help in preparation of the figures and W. Marshall for typing the manuscript. Jerry Mahlman, Director of the Geophysical Fluid Dynamics Laboratory has encouraged and supported this project and generously allocated the computer resources needed to complete the calculations.

REFERENCES

Bacastrow, R., and A. Bjorkstrom, 1981: Comparison of ocean models for the carbon cycle. *Carbon Cycle Modeling.* B. Bolin, Ed., *SCOPE,* Wiley and Sons, **16,** 29–80.

Bryan, K., 1969: Climate and the ocean circulation: III. The ocean model. *Mon. Wea. Rev.,* **97,** 806–827.

——, 1984: Accelerating the convergence to equilibrium of ocean–climate models. *J. Phys. Oceanogr.,* **14,** 666–673.

——, and L. J. Lewis, 1979: A water mass model of the World Ocean. *J. Geophys. Res.,* **84**(C5), 2503–2517.

——, and M. J. Spelman, 1985: The ocean's response to a carbon dioxide-induced warming. *J. Geophys. Res.,* **90**(C6), 11 679–11 688.

——, S. Manabe and R. C. Pacanowski, 1975: A global ocean-atmosphere climate model. Part II. The oceanic circulation. *J. Phys. Oceanogr.* **5,** 30–46.

——, F. G. Komro, S. Manabe and M. J. Spelman, 1982: Transient response to increasing atmospheric carbon dioxide. *Science* **215,** 56–58.

Cess, R. D., and S. D. Goldenberg, 1981: The effect of the ocean heat capacity upon global warming due to increasing atmospheric carbon dioxide. *J. Geophys. Res.,* **86,** 498–502.

Deacon, G. E. R., 1937: Note on the dynamics of the southern ocean. *Discovery Reports,* Cambridge University Press, **15,** 125–152.

Gill, A. E., and K. Bryan, 1971: Effects of geometry on the circulation of a three dimensional southern-hemisphere ocean model. *Deep-Sea Res.,* **18,** 685–721.

Gordon, A., 1982: Weddell Sea deep water variability. *J. Mar. Res.,* **40**(Suppl.), 199–217.

Hansen, J., A. Lacis, D. Rind, G. Russell, P. Stone, I. Fung, R. Ruedy and J. Lerner, 1984: Climate sensitivity: Analysis of feedback mechanisms. *Climate Processes and Climate Sensitivity, Geophys. Monogr. 29 Maurice Ewing,* Vol. 5, J. E. Hansen and T. Takahashi, Eds., AGU, **5,** 130–163.

Harvey, L. D. D., and S. H. Schneider, 1985: Transient climate response to external forcing on 10^0–10^4 year time-scales. Part II. *J. Geophys. Res.,* **90**(D1), 2207–2222.

Hoffert, M. I., A. J. Callegari and C.-T. Hsieh, 1980: The role of deep sea storage in the secular response to climate forcing. *J. Geophys. Res.,* **85,** 6667–6679.

Jones, P. D., T. M. L. Wigley and P. B. Wright, 1986: Global temperature variations between 1861 and 1984. *Nature,* **322,** 430–434.

Levitus, S., 1982: *Climatological Atlas of the World Ocean,* NOAA Prof. Paper 13, U.S. Dept. Commerce, Washington, DC, 173 pp.

Manabe, S., 1969: Climate and ocean circulation. II: Atmospheric circulation and the effect of heat transport by ocean currents. *Mon. Wea. Rev.,* **97,** 775–805.

——, and R. Wetherald, 1967: Thermal equilibrium of the atmosphere with a given distribution of relative humidity. *J. Atmos. Sci.,* **24,** 241–259.

——, and K. Bryan, 1969: Climate calculations with a combined ocean–atmosphere model. *J. Atmos. Sci.,* **26,** 786–789.

——, and R. Wetherald, 1975: The effects of doubling the CO_2 concentration on the climate of a general circulation model. *J. Atmos. Sci.,* **32,** 3–15.

——, and K. Bryan, 1985: CO_2-induced change in a coupled ocean-atmosphere model and its paleoclimatic implications. *J. Geophys. Res.,* **90**(C11), 11 689–11 707.

——, —— and M. J. Spelman, 1975: A global ocean-atmosphere climate model. Part I: The atmospheric circulation. *J. Phys. Oceanogr.,* **5,** 3–29.

McCartney, M. S., 1977: Subantarctic mode water. Contribution to *George Deacon: 20th Anniversary Volume,* M. V. Angel, Ed., Pergamon, 103–119.

Oort, A. H., 1983: *Global Atmospheric Circulation Statistics,* 1958–1973. NOAA Prof. Paper 14, U.S. Dept. Commerce, Washington DC, 180 pp.

Sarmiento, J. L., 1983: A simulation of bomb-trituim entry into the Atlantic Ocean. *J. Phys. Oceanogr.,* **13**(10), 1924–1939.

Schlesinger, M. E., and X. Jiang, 1987: The transport of CO_2-induced warming into the ocean: An analysis of simulations by the OSU coupled atmosphere-ocean general circulation model. *Climate Dynamics,* in press.

——, W. L. Gates and Y.-J. Han, 1985: The role of the ocean in CO_2-induced climatic warming: Preliminary results from the OSU coupled atmosphere-ocean GCM. *Coupled Ocean-Atmosphere Models,* J. C. J. Nihoul, Ed., Elsevier, 447–478.

Spelman, M. J., and S. Manabe, 1984: Influence of oceanic heat transport upon the sensitivity of a model climate. *J. Geophys. Res.,* **89,** 571–586.

Thompson, S. L., and S. H. Schneider, 1982: Carbon dioxide and climate: The importance of realistic geography in estimating the transient temperature response. *Science,* **217,** 1031–1033.

Whitworth, T. III, 1983: Monitoring the transport of the Antarctic Circumpolar Current at the Drake Passage. *J. Phys. Oceanogr.,* **13**(11), 2045–2057.

Wigley, T. M. L., and M. E. Schlesinger, 1985: Analytical solution for the effect of increasing CO_2 on global mean temperature. *Nature,* **315,** 649–652.